Revista Biomédica

https://revistabiomedica.mx

Artículo original

Environmentally Friendly Low-Temperature Synthesis of Black TiO_2 Nanoparticles and Preliminary Cytotoxicity Evaluation in HEK-293T Cells

Angel Daniel Ramírez-Herrera[1], Luis Alberto Bretado-Aragón[2*], Gloria Barbosa-Sabanero[3], Yolanda Alvarado-Caudillo[3], Yvain de los Ángeles Salinas-Delgado[2], Luis Fernando Ceja-Torres[1].

[1]Instituto Politécnico Nacional, Centro Interdisciplinario de Investigación para el Desarrollo Integral Regional Unidad Michoacán, Jiquilpan, Michoacán 59510, México. [2]Ingeniería en Nanotecnología, Universidad de La Ciénega del Estado de Michoacán de Ocampo, Sahuayo, Michoacán 59103, México. [3]Departamento de Ciencias Médicas, Universidad de Guanajuato, León, Guanajuato 37320, México.

RESUMEN

Síntesis ecológica a baja temperatura de nanopartículas de TiO_2 negro y su evaluación preliminar de citotoxicidad en células HEK-293T

Introducción. El TiO_2 se utiliza en diversas aplicaciones y dispositivos médicos. Sus propiedades específicas, incluida su banda prohibida, desempeñan un papel fundamental en las aplicaciones médicas. El TiO_2 se utiliza ampliamente en aplicaciones biomédicas por su capacidad para reflejar y dispersar la radiación UV, así como por sus propiedades antimicrobianas.

Objetivo. Este estudio tuvo como objetivo informar sobre un método ecológico, de baja temperatura y rápido para sintetizar $BTiO_2$NPs y evaluar su citotoxicidad en células renales embrionarias humanas.

Métodos. Para la síntesis se utilizó un medio acuoso, ácido ascórbico y $TiCl_3$. Las nanopartículas se caracterizaron mediante difracción de rayos X, microscopio electrónico de barrido, espectroscopia de energía dispersiva, espectroscopia infrarroja por transformada de Fourier y espectrometría UV-Vis. La citotoxicidad de las nanopartículas de $BTiO_2$NPs se analizó con los ensayos de exclusión de azul tripano y XTT.

Resultados. El tamaño de cristalita obtenido para la fase anatasa fue inferior a 10 nm, con morfología esférica y superficies deficientes en oxígeno. También se pudo formar una fase amorfa de TiO_2 con exceso de $TiCl_3$. La misma síntesis sin ácido ascórbico dio como resultado una fase de rutilo con tamaño nanométrico. Se obtuvo más del 80% de viabilidad en células HEK-293T en todos los tratamientos; hubo un efecto mínimo dependiente del tiempo y la concentración en la viabilidad y proliferación celular, lo que indica baja citotoxicidad.

Historial del artículo
Recibido: 19 mar 2025
Aceptado: 11 jun 2025
Disponible en línea: 1 sep 2025

Palabras clave
Síntesis a baja temperatura, TiO_2 negro, Citotoxicidad, Células HEK-293T, Síntesis ecológica.

Keywords
Low-temperature synthesis, Black TiO_2, Cytotoxicity, HEK-293T cells, Eco-friendly synthesis

Copyright © 2025 por autores y Revista Biomédica.
Este trabajo está licenciado bajo las atribuciones de la *Creative Commons* (CC BY).
http://creativecommons.org/licenses/by/4.0/

*Autor para correspondencia:
Luis Alberto Bretado-Aragón, Universidad de La Ciénega del Estado de Michoacán de Ocampo, Sahuayo, Michoacán 59103, México.
ORCID: https://orcid.org/0000-0001-6167-5501
E-mail: labretado@ucemich.edu.mx.
https://revistabiomedica.mx.

Conclusión. Se obtuvieron nanopartículas de TiO_2 modificadas superficialmente con tamaños inferiores a 100 nm. Se demostró una citotoxicidad baja en HEK-293T, pero un aumento del metabolismo mitocondrial. Este nanomaterial se presenta prometedor para aplicaciones biomédicas, a la espera de estudios adicionales.

ABSTRACT

Introduction. Titanium dioxide (TiO_2) finds use in various medical applications and devices. Its unique properties, particularly its band gap, play a key role in these applications. TiO_2 is widely employed in biomedical contexts due to its capability to reflect and scatter UV radiation, as well as its antimicrobial properties.

Objective. This study aimed to present an eco-friendly, low-temperature, and rapid method for synthesizing black titanium dioxide nanoparticles ($BTiO_2$NPs) and to evaluate their cytotoxicity in human embryonic kidney cells.

Methods. An aqueous medium, ascorbic acid, and titanium chloride ($TiCl_3$) were utilized for the synthesis. Nanoparticles were characterized using X-ray diffraction (XRD), scanning electron microscopy (SEM), energy-dispersive spectroscopy (EDS), Fourier-transform infrared spectroscopy (FTIR), and UV-Vis spectrometry. The cytotoxicity of $BTiO_2$NPs was evaluated with the trypan blue exclusion and XTT assays.

Results. The obtained anatase had a crystallite size of under 10 nm, exhibiting a spherical morphology and oxygen-deficient surfaces. With excess $TiCl_3$, an amorphous TiO_2 phase could also form. The same synthesis without ascorbic acid yielded a rutile phase with a nanometric size. Over 80% viability was achieved in HEK-293T human embryonic kidney cells (HEK-293 T, CRL-3216 ATCC) across all treatments; a minimal time- and concentration-dependent effect on cell viability and proliferation was noted, indicating low cytotoxicity.

Conclusion. Surface-modified TiO_2 nanoparticles smaller than 100 nm were produced. They exhibited low cytotoxicity in human kidney cells (HEK-293T) while enhancing mitochondrial metabolism. Further studies are needed on this nanomaterial, which shows potential for biomedical applications.

INTRODUCTION

TiO_2 is a metal oxide that occurs naturally and is widely used in industrial and commercial products. It possesses various attractive and beneficial properties, for example, thermal stability, photocatalytic potential, and resistance to ultraviolet radiation, which can vary depending on the material's primary particle size, crystallinity, and formulation (1). This has led to efforts to dope TiO_2 with other chemical elements that alter its chemical structure and size, such as black titanium ($BTiO_2$) (2). $BTiO_2$ exhibits a thin amorphous shell around the crystal lattice that contributes to the decrease in its crystallinity, which is optically noticeable by the change in its coloration and can depend on the degree of reduction and defects (3). $BTiO_2$ nanoparticles ($BTiO_2$NPs) have gained significant attention since 2011, particularly for their enhanced photocatalytic and biomedical applications, due to their modified electronic and surface properties. Specifically, $BTiO_2$NPs demonstrate various therapeutic and diagnostic properties that make them ideal for biomedical applications (4) due to different structural and chemical modifications, including oxygen/Ti^{3+} vacancies, additions of hydroxyl groups, and Ti–H bonds (3).

However, no consensus exists among the various synthetic methodologies developed regarding the specific conditions or equipment best suited for obtaining $BTiO_2$NPs (5). Most of the syntheses reported in the literature employ highly toxic reducing agents (e.g., $NaBH_4$) or specific conditions for their production, controlled atmosphere and heat treatment (5). Another option is the prior preparation of nanoparticles for subsequent reduction using sophisticated equipment (6). Some research continues to explore a simple and environmentally friendly method; several approaches have been attempted toward this goal. For instance, Shah *et al*. (7) synthesized $BTiO_2$NPs using a hydrothermal process at relatively low temperatures (180°C) and with environmentally safe chemicals, similar to ascorbic acid. However, further research is still needed in this area.

A simple and environmentally friendly method is necessary because a significant portion of the observed cytotoxicity in nanomaterials is often attributed to the presence of residual reagents from their synthesis, such as metal ions, reducing agents, or surface-active compounds used in their production (8). An example of this was reported by Prokopiuk *et al.* (9), which demonstrated that $BTiO_2$NPs exhibit low toxicity against primary fibroblasts but induce reactive oxygen species and Ca^{2+} mediated eryptosis, indicating a latent risk of the particles towards other cell lines. In contrast, Ni *et al.* (10), who utilized the low band gap of $BTiO_2$NPs triggered by near-infrared light, emphasized the destructive effect on bladder cancer cells, exhibiting low toxicity, good biocompatibility, and a high anticancer effect *in vitro*. Additionally, Sun *et al.* (11) reported that $BTiO_2$NPs settled in vesicles within the cytoplasm of HeLa cells through endocytosis, which, when subjected to irradiation, induces severe cell death with a photothermal conversion efficiency as much as 204% higher than other types of TiO_2. There are extensive studies on the vulnerability of cancer cells to the photocatalytic effects of TiO_2 nanoparticles (NPs), where the mechanisms of action are directly related to genotoxicity induced by DNA damage (12). Although TiO_2 cytotoxicity has been thoroughly studied in cancer cell lines, its effects on non-cancerous human cell models, particularly regarding the newly engineered $BTiO_2$NPs, remain relatively unexplored. TiO_2NPs have been shown to generate oxidative stress, apoptosis, inflammatory responses, and genotoxicity, as well as causing neurotransmitter deregulation, altering the distribution of trace elements, and interfering with signaling pathways, which has led to its ban in some countries as a food additive (13).

Given the above considerations, it is necessary to establish simple techniques that produce little or no harm to the environment and human health. It is imperative to find a synthesis method for $BTiO_2$NPs that does not use or generate toxic compounds, increasing the toxicity of the nanomaterial, such as using ascorbic acid as a reducing agent. Furthermore, analyzing these synthesized nanomaterials is required to ensure the ideal synthesis route. Therefore, the current contribution describes a simple one-step process for synthesizing $BTiO_2$NPs at an even lower reaction temperature and without any catalysts or controlled atmosphere. In addition, the cytotoxic potential of nanomaterials, of which there are few reports in the literature, was analyzed to ensure their safe use and enhance knowledge surrounding this novel material.

MATERIALS AND METHODS

Synthesis of TiO_2 NPs

$TiCl_3$ (≥ 12% in HCl, Sigma-Aldrich), ascorbic acid (99% purity, Meyer), and deionized water were used. A 0.3 M solution of ascorbic acid (150 ml) was prepared in deionized water at 60°C with constant stirring (700 rpm) under a fume hood, adding 10 ml of the $TiCl_3$ solution dropwise. The solution's pH (approximately 2) at both the beginning and end of the synthesis was not changed. After this process, the solution was restated and placed in an oven at 60°C to remove the solvent. The resulting material was washed with deionized water and dried at 60°C. The obtained powder was stored in a desiccator for later use. The same procedure was performed without ascorbic acid and with an excess of $TiCl_3$ in solution.

Characterization of TiO_2 NPs

The phase analysis was conducted using X-ray diffraction with a D8 Advance A25 apparatus (Bruker) under the following conditions: CuKα radiation (0.15405 nm), with an initial angle of 20° and a final angle of 79.99°, a scan step of 0.00409206°, a voltage of 30 kV, and a current intensity of 20 mA. The crystallite size was determined using the Scherrer equation. Morphological analysis was performed with an SEM equipped with EDS (JEOL 66-10LV, JEOL), using 20 kV, a working distance of 10 mm, and gold-coated samples. Functional groups were examined using FTIR spectroscopy (Frontier, Perkin Elmer) at a wavelength range from 4000 to 400 cm^{-1}. Optical properties were assessed using UV-Vis spectroscopy (Lambda 25, Perkin Elmer) at 200 to 800 nm wavelengths.

Cell cultures for cytotoxicity assays

Human embryonic kidney cells (HEK-293 T, CRL-3216, ATCC) were exposed to $BTiO_2$NPs to assess cytotoxicity. According to the supplier, they were cultivated at 37°C for 72 h with 100% humidity and a 5%CO_2 concentration, using Dulbecco's Modified Eagle Medium (DMEM) (Gibco-Invitrogen) with low glucose and glutamine levels, supplemented with sodium pyruvate (110 mg/ml), 10% fetal bovine serum, 100 U/ml of penicillin, and 100 µg/ml of streptomycin. After 72 h, HEK-293 T cells formed a monolayer, which was trypsinized by incubating the cells with a 0.05% trypsin/EDTA solution at 37°C for 5 min. The cell suspension was centrifuged at 1200 rpm for 5 min, and the cell pellet was resuspended in 1 ml of complete medium. Before the studies, the $BTiO_2$NPs were suspended by sonication for 20 min in the enriched DMEM mentioned above. The cell suspension with varying concentrations of $BTiO_2$NPs (0, 25, 50, 100, 200, and 400 µg/ml) was added to a 96-well plate ($1x10^5$ cells/ml) for the XTT (2,3-Bis-(2-Methoxy-4-Nitro-5-Sulfophenyl)-2H-Tetrazolium-5-Carboxanilide) colorimetric cell viability assay or to 6-well plates (2x105 cells/ml) for the trypan blue exclusion assay.

Cell viability assays

Regarding the latter, after incubation with $BTiO_2$NPs, cells in the 6-well plates were washed with NaCl (0.9%). The cell solution was centrifuged at 1200 rpm for 5 min, and the supernatant was discarded. The cell pellet was resuspended in 1 ml of medium, and the resulting suspension (95 µl) was stained with 5 µl of trypan blue (0.4%). Cell viability was assessed under a Motic digital light microscope.

Cell proliferation assays

The XTT assay was conducted following the manufacturer's instructions (Sigma-Aldrich) after 24 and 48 h of exposure to $BTiO_2$NPs. Blanks were prepared for each $BTiO_2$NP treatment, considering the absorption and degradation of XTT salts, to adjust the results obtained. Absorbance measurements (490 nm) were taken using a microplate spectrophotometer (Multiskan Go, Thermo Scientific) at these two time points. Each exposure duration was assessed in triplicate during the viability and proliferation assays.

Statistical analysis

In all cases, the normality and homogeneity of variance requirements were analyzed. The experimental design was conducted using completely randomized blocks. A one-way analysis of variance (ANOVA) with a *post hoc* Tukey test was performed to compare statistical differences. The significance level used was $p < 0.05$.

RESULTS

The addition of $TiCl_3$ caused an immediate reaction, triggering a change from a colorless solution to a dark orange/reddish one (Figure 1, bottom) and producing gas. By the end of the response, only a light orange residue was found in the samples with excess $TiCl_3$. The nanoparticles were separated by centrifugation and treated in the same process as the $BTiO_2$NPs (Figure 1, top and middle). Interestingly, the residue was directly proportional to the amount of $TiCl_3$ added, being almost negligible with a 10 ml volume.

XRD confirmed the presence of TiO_2 in the samples. The orange precipitate (Figure 1, middle) displayed broad, low-intensity peaks with poor crystallization and amorphous material, representing the entire diffraction pattern. In contrast, the wide, low-intensity peaks of $BTiO_2$NPs (Figure 1, bottom) showed good crystallization, characteristic of the anatase phase (JCPDS card No. 00-002-0406). The diffracted peaks at 2θ correspond to 25.17°, 37.67°, 47.85°, 53.96°, 62.37°, 68.69°, and 74.89°, associated with the (1 0 1), (0 0 4), (2 0 0), (1 0 5), (2 0 4), (1 1 6), and (2 1 5) planes, respectively. The space group belongs to tetragonal I 4_1/amd (No. 141) with lattice parameters calculated for a, b equal to 3.79 Å and c equal to 9.52 Å. Conversely, white titanium dioxide ($WTiO_2$) (Figure 1, top) exhibited broad, low-intensity, crystalline peaks typical of the rutile phase (JCPDS card No. 01-0781510). The diffracted peaks at 2θ correspond to 27.35°, 36.08°, 39.06°, 41.21°, 43.90°, 54.22°, 56.44°, 62.86°, and

69.85°, associated with the (1 1 0), (1 0 1), (2 0 0), (1 1 1), (2 1 0), (2 2 0), (0 0 2), and (1 1 2) planes, respectively. The space group belongs to tetragonal P 4_2/mnm (No. 136) with lattice parameters calculated for a, b equal to 4.60 Å and c equal to 2.95 Å. The crystallite size of the various forms of TiO_2 was determined using the Scherrer equation. The Scherrer equation for calculating particle size is $D=(K\lambda)/(\beta\cos\theta)$; where K is the Scherrer constant, commonly valued at 0.9, λ is the wavelength of the X-ray beam used (1.5418 Å), β is the full width at half maximum (FWHM) of the peak, and θ is the Bragg angle (14). The Scherrer equation accounts for broadening solely due to crystallite size. The sizes of $BTiO_2$NPs and $WTiO_2$ calculated from the main peaks were 10.07 ±4.71 nm and 20.77 ±7.89 nm, respectively.

Regarding the SEM results (Figure 2A, B, and C), some agglomerates of quasi-spherical and amorphous particles were observed, with sizes well under 100 nm. In the EDS study (Figures 2D, E, and F), there were peaks corresponding to titanium and oxygen were observed. Additional evidence indicates the presence of C and Cl atoms from ascorbic acid and residues or impurities. FTIR spectroscopy showed various peaks, some attributed to the vibrational modes of OH groups at 3200-3600 cm^{-1} and 1700-1600 cm^{-1} (Figure 3).

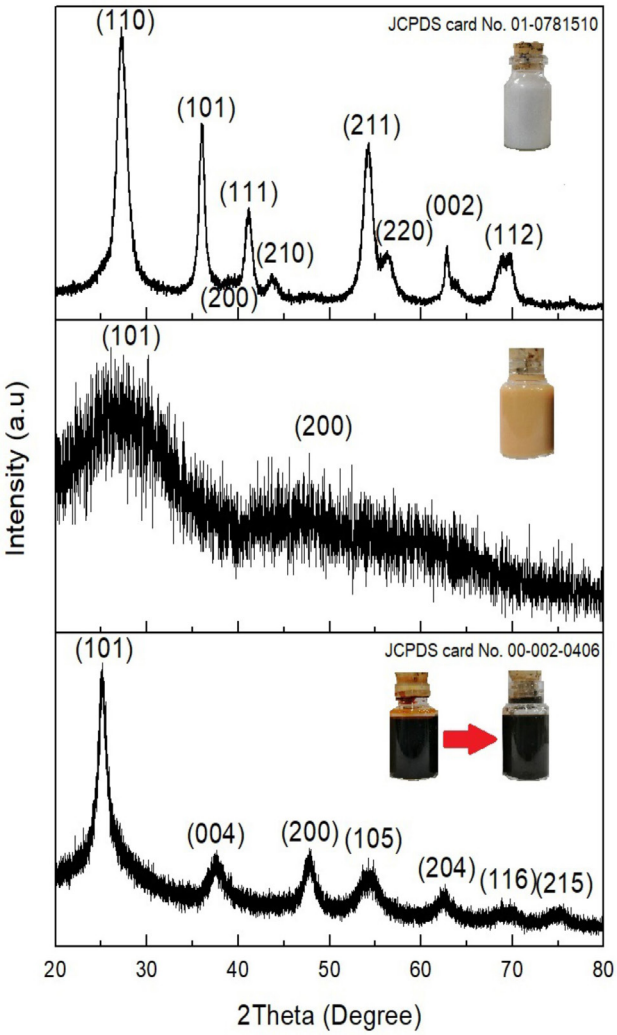

Figure 1. XRD patterns (top to bottom) of $WTiO_2$, amorphous TiO_2, and $BTiO_2$NPs, respectively.

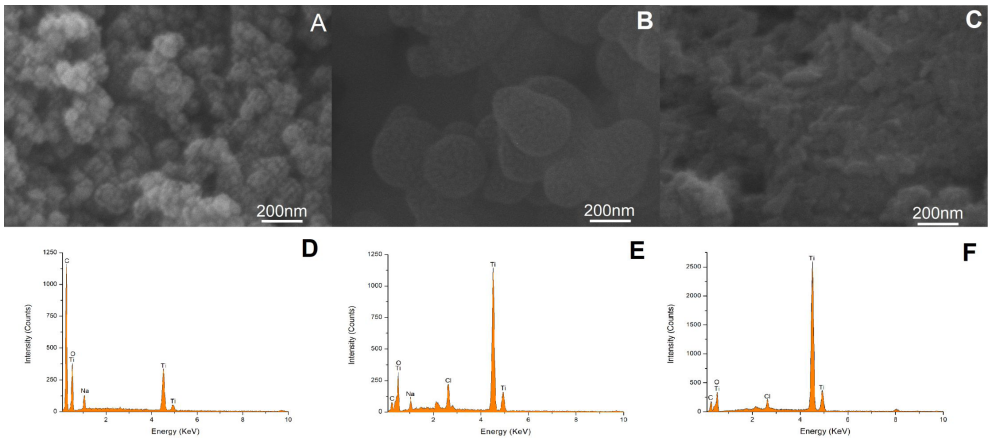

Figure 2. Scanning electron microscopic micrographs and their corresponding EDS for amorphous TiO_2 (A and D), $BTiO_2$NPs (B and E), and $WTiO_2$ (C and F).

The presence of ascorbic acid in the NPs is indicated by peaks from its carbonyl groups and other peaks belonging to the same molecule (Figure 3, top). A clear difference is observed in the FT-IR spectra between the $WTiO_2$ and those synthesized with ascorbic acid, in the range of 1600 to 1100 cm^{1}, indicative of the residues of the aforementioned carbonyl groups. Moreover, the inverted peak at 1000 cm^{-1} suggests the bonding between Ti-O-O-C (15). The presence of the TiO_2 band is noted in the wave range of 400 to 800 cm^{-1}. A broader band observed from 400 to 1000 cm^{-1} can be attributed to the Ti-O and Ti-O-Ti bridging stretching modes. Regarding the UV-Vis spectrum, a peak of excellent absorption intensity appears at around 300 nm (Figure 3, middle). The optical band gap was determined using the Tauc plot method (16), yielding 3.38 eV for $BTiO_2$NPs and 3.59 eV for $WTiO_2$ (Figure 3, bottom).

The cell viability study revealed no damaged or dead cells with trypan blue staining across all treatments and times analyzed. However, increasing the concentration of $BTiO_2$NPs also led to enhanced sedimentation and a significant amount of cellular agglomeration attached to them. A key point to note is the affinity of the $BTiO_2$NPs to attach exclusively to cell membranes, avoiding areas where they did not develop, suggesting that the surface charge of both the cell membrane and the $BTiO_2$NPs contributed to this agglomeration. This could facilitate potential internalization into cells (Figure 4). The decrease in cell viability of HEK 293T (Figure 5A) depends on the concentration and exposure time. The 100 µg/ml concentration shows statistically significant differences compared to the control at both exposure times. In contrast, 400 µg/ml concentration only shows this effect after 48 h of exposure, although all treatments maintained over 85% viability. Furthermore, in this graph, at 24 h, there is a trend toward increased viability, even surpassing the control.

Subsequently, it declines, contrasting with the 48 h of exposure, which generally shows a decrease. The IC_{50} calculated for the 24-h treatment was 1389 µg/ml, whereas for the 48-h treatments it was 1277 µg/ml. As demonstrated, the $BTiO_2$NPs did not exhibit a significant decrease in cell viability at the concentrations and cell line used.

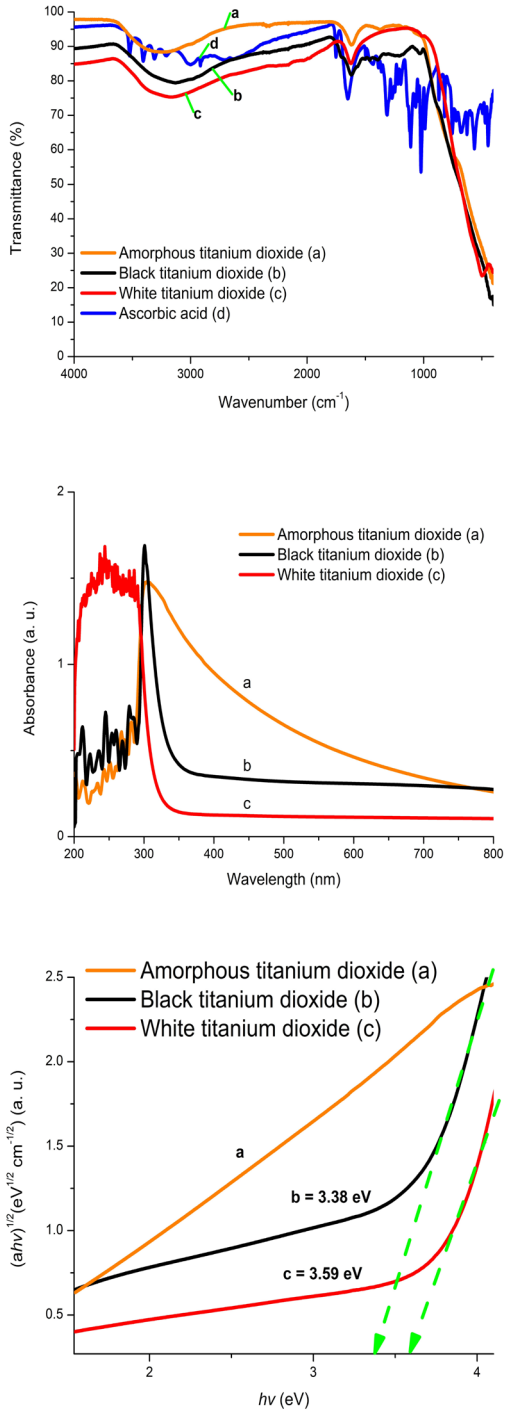

Figure 3. FT-IR spectra (top), UV-Vis spectra (middle), and Tauc plot (bottom) of amorphous TiO_2 (a), $BTiO_2$NPs (b), $WTiO_2$ (c), and ascorbic acid (only FT-IR spectra).

 https://doi.org/10.32776/revbiomed.v36i3.1342

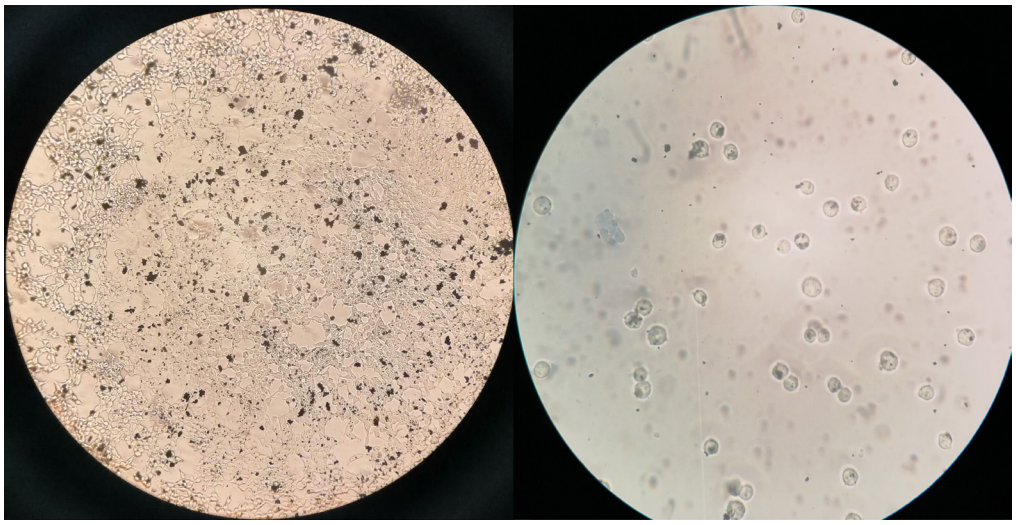

Figure 4. Deposition of nanoparticles in the 100 µg treatment before (10x, left) and during (40x, right) the trypan blue exclusion assay counting.

On the other hand, in the proliferation tests where mitochondrial activity was measured through the degradation of XTT, greater activity was observed compared to the control in all samples. However, only the 400 µg/ml concentration showed a statistically significant difference at 24 h of exposure (Figure 5B). Therefore, based on the obtained results, it can be stated that $BTiO_2$NPs cause HEK 293T cells to be metabolically more active, depending on the concentration and exposure time, even though there is less cellular presence. The increased mitochondrial activity induced by $BTiO_2$NPs may be attributed to the defense mechanisms of HEK cells against particle-mediated cellular stress.

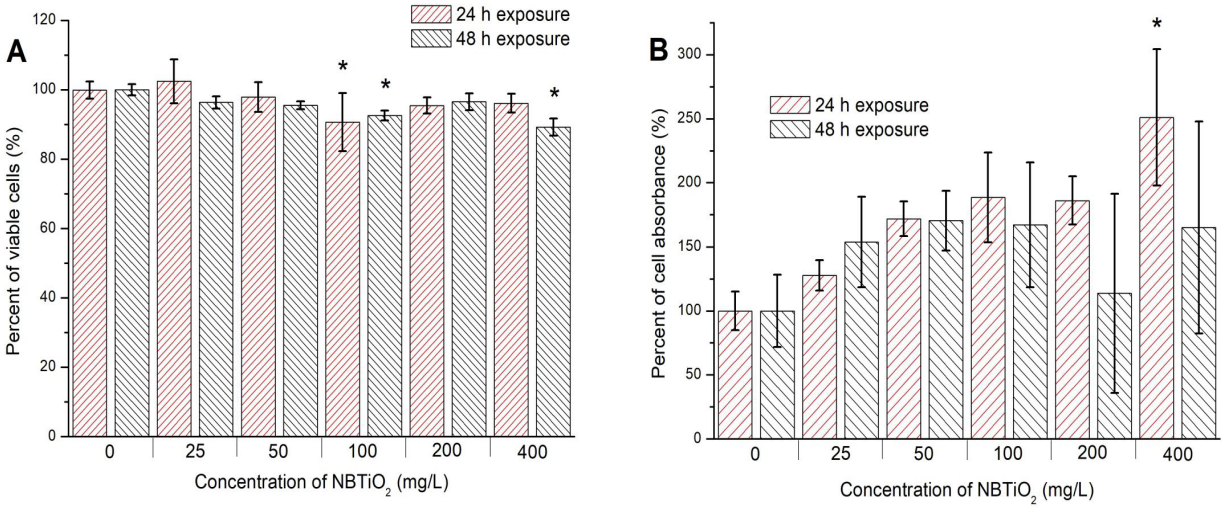

Figure 5. Trypan blue exclusion (A) and XTT (B) assays. Values represent the mean ± SD of three or more independent experiments. * Statistical differences ($p<0.05$ versus the control) based on one-way ANOVA and the Tukey test.

DISCUSSION

The previous synthesis reaction varies from that described by Shah *et al*. (7), who observed a purple solution after mixing ascorbic acid with different concentrations of $TiCl_3$ at room temperature. Therefore, temperature is crucial for the one-step formation of $BTiO_2$NPs. When titanium atoms react with ascorbic acid, their binding to electron-donating ligands facilitates the formation of complexes and changes in coloration (17), which the following equations can illustrate:

$$C_5H_5O_5CH_2OH + H_2O + TiCl_3 \xrightarrow{\Delta} HCl\uparrow + (C_5H_5O_5CH_2O)_3Ti + \text{Ti oxo species} \quad (1)$$

$$(C_5H_5O_5CH_2O)_3Ti + \text{Ti oxo species} \xrightarrow{\Delta} TiO_2 \quad (2)$$

The first reaction occurs instantaneously (Eq. 1). The hydrolysis of $TiCl_3$ produces hydrochloric acid and several intermediate titanium compounds between TiO_2^+ and TiO_2. Finally, the nucleation process yields titanate with an oxygen-deficient surface (Eq. 2).

Adding $TiCl_3$ to a solution without ascorbic acid also produced an immediate reaction, resulting in a milky white color, gas formation, and the synthesis of white titanium dioxide ($WTiO_2$). The following equation can explain this:

$$H_2O + TiCl_3 \xrightarrow{\Delta} HCl\uparrow + \text{Ti oxo species} \quad (3)$$

$$\text{Ti oxo species} \xrightarrow{\Delta} TiO_2 \quad (4)$$

The orange precipitate of amorphous TiO_2 belongs to an anatase structure, as Dai *et al*. (18) reported. In contrast, Pedraza and Vazquez (19) obtained rutile through a similar process, which required more time and thermal treatments to achieve the desired crystallization compared to the current procedure due to their experimental conditions. Consistent with previous studies, ascorbic acid did not affect the crystal structure (20). However, this lack of effect from ascorbic acid can be attributed to the working temperature. At temperatures above 70°C, rutile phase crystallites with a higher surface free energy may promote anatase phase crystallization.

The findings in the FTIR spectra resemble those reported by Chen *et al*. (21), who also worked with $BTiO_2$NPs. Additionally, the UV-Vis spectrum peak around 300 nm can be attributed to the band gap interval of the crystalline phase of the particles (19). The spectrum is similar to that published by Su *et al*. (22), who detected a linear behavior in the visible spectrum and an absorption band at 300 nm, as well as a band gap calculated by the Tauc plot method for $BTiO_2$NPs.

One significant limitation of this study is that the zeta potential and colloidal stability of the $BTiO_2$NPs were not measured. Therefore, we cannot ensure the correct dispersion of the solutions and the electrostatic affinity between $BTiO_2$NPs and cells. In addition to this, the internalization into cells is a highly complex process, determined by the properties of the material (particle size, shape, morphology, crystalline structure, and surface charge) as well as the characteristics of the cell (membrane structure, segregated molecules, surface charge, etc.) (23). The effect reported by Filippi *et al*. (24) is called "Trojan Horse," which occurs when particles are deposited on the surface of a cell and then enter via diffusion, endocytosis, or pinocytosis, without control over intracellular concentration. This phenomenon may be happening in this study, given the apparent affinity of the NPs for this cell line. Additionally, a study by Meena *et al*. (25), involving TiO_2 NPs on HEK 293T cells, reports internalization and even interaction of the particles with the nuclear membrane, leading to apoptotic characteristics in the treated cells. The mechanism by which these particles induce damage has not yet been clarified (23, 25). It has been proposed that the potential mechanisms of action causing cytotoxicity are associated with generating reactive oxygen species (ROS) and damage due to oxidative stress (24). The increase in mitochondrial activity could be linked to compensatory mechanisms in response to cellular stress. However, given the analyses' limitations, it is difficult to assert that this effect occurs in the present work. Further study of ROS generation, apoptosis, and validation in other cellular models or in vivo systems is needed. Nevertheless, the observed cellular decline alongside increased activity of HEK 293T cells (Figure 4) indicates the presence of cellular stress

in this study, necessitating apoptosis analysis and direct measurement of ROS to clarify the action pathway of the NPs.

Furthermore, the formation of superoxides generated by $BTiO_2$NPs is possible, which could lead to a false positive by increasing cell proliferation, as mentioned by Wang *et al*. (26). However, the effect of $BTiO_2$NPs on XTT salts due to superoxides was managed because when the superoxides generated by $BTiO_2$NPs interact with XTT, they are reduced to generate formazan. This effect is accounted for by bleaching each of the samples without cells, a process that was conducted. Therefore, this increase in cell viability cannot be attributed solely to superoxides. Tucci *et al*. (27) demonstrated that the effect of TiO_2 NPs does not necessarily impact the phases of the cell cycle or issues related to cell death; instead, the NPs affect mitochondrial activities. They found that at high doses (100 µg/ml) after 24 h of exposure, metabolic alterations increased in eighty-five biochemical compounds, many associated with the cellular stress response. Another study by Bo *et al*. (28) indicates that TiO_2 can trigger damage to energy processes while inhibiting the synthesis of ribonucleic acid and deoxyribonucleic acid, as it interferes with the metabolic pathways of specific amino acids, L-aspartate and L-β-alanine. Similarly, Valentini *et al*. (29) report observing changes in various substances involved in energy generation, such as the Krebs cycle, which promotes an increase in primary compounds in this cycle. These changes reflect a transient process of cellular metabolism that quickly counteracts the effects of oxidative stress, ultimately resulting from an increase in the enzymatic and metabolic machinery present not only in the mitochondria but throughout the cell.

The enhancement of the catalytic properties of $BTiO_2$ closely relates to the formation of structural defects, primarily oxygen vacancies and Ti^{3+} states within its crystal lattice. These defects introduce intermediate energy levels within the bandgap, effectively narrowing it and allowing the absorption of lower-energy photons, thus extending its activity into the visible and near-infrared regions (30). Furthermore, an increase in charge carrier density and improved charge separation have been observed due to efficient electron trapping (31). As a result, the photocatalytic activity of $BTiO_2$NPs is significantly enhanced due to its greater light-harvesting capacity and charge separation efficiency.

Due to these improved properties, $BTiO_2$ shows great potential in various biomedical and environmental applications. For example, Photodynamic Therapy (PDT) allows $BTiO_2$ to act as a photocatalyst that generates ROS, selectively destroying cancer cells under light irradiation (32). Photothermal Therapy (PTT) efficiently converts light energy into heat, enabling the thermal ablation of cancerous cells. Reported photothermal conversion efficiencies are as high as 40.8%, coupled with low toxicity. NIR light-activated PTT has proven effective *in vivo* tumor ablation (33). On the other hand, $BTiO_2$ demonstrates superior photocatalytic degradation of bacteria under UV and visible light compared to $WTiO_2$ (34). Its antibacterial activity can be further enhanced by incorporating nanostructures or doping materials. $BTiO_2$NPs are suitable for electrochemical and photoelectrochemical biosensors (PEC) applications, offering high sensitivity for detecting microRNAs and other biomarkers, making it a promising platform for advanced diagnostic technologies (35).

CONCLUSIONS

A fast and simple method for preparing $BTiO_2$NPs and nanoparticles with minimal reduction in viability is described here. The obtained nanoparticles exhibit a single anatase phase (using ascorbic acid) or the rutile phase (without the stabilizer). They measure less than 100 nm in diameter and demonstrate potential for surface functionalization with ascorbic acid. During synthesis, the presence of ascorbic acid influenced the resulting crystal structure. Moreover, the limited effect of these nanoparticles on cell viability was only observed at concentrations of

100 and 400 mg/L, yet cell viability remained above 85%. The treatments encouraged an increase in cell metabolism. However, further experimental research is needed to confirm their safety and to explore potential applications, such as characterizing the nanoparticle surfaces and investigating the mechanisms of action at the mitochondrial level across different cell lines. Due to their tunable properties and safe origin, $BTiO_2$NPs can be a biofunctional biomedical material. With ongoing research and technological innovation, we believe this nanomaterial will advance the field of biomedicine.

Ethical statement

The tests with HEK 293T cells (CRL3216-ATCC) were carried out following the supplier's instructions, and strict internationally approved protocols and procedures were followed before, during, and after the test.

REFERENCES

1. Ayorinde T, Sayes CM. An updated review of industrially relevant titanium dioxide and its environmental health effects. JHM Letters 2023 Nov; 4: 1-7. https://doi.org/10.1016/j.hazl.2023.100085
2. Andronic L, Enesca A. Black TiO_2 Synthesis by Chemical Reduction Methods for Photocatalysis Applications. Front. Chem. 2020 Nov; 8: 1-8. https://doi.org/10.3389/fchem.2020.565489
3. Tuntithavornwat S, Saisawang C, Ratvijitvech T, Watthanaphanit A, Hunsom M, Kannan AM. An extensive review of the recent development of black TiO_2 nanoparticles for photocatalytic H_2 production. Int. J. Hydrogen Energy 2024 Feb; 55: 1559-1593. https://doi.org/10.1016/j.ijhydene.2023.12.102
4. Kafshgari MH, Goldmann WH. Insights into Theranostic Properties of Titanium Dioxide for Nanomedicine", Nano-Micro Lett. 2020 Jan; 12(22): 1-35. https://doi.org/10.1007/s40820-019-0362-1
5. Selema TC, Malevu TD, Mhlongo, MR, Motloung SV, Motaung TE. Advancements in black titanium dioxide nanomaterials for solar cells: a comprehensive review. Emergent mater. 2024 May; 7, 2163–2188. https://doi.org/10.1007/s42247-024-00731-z
6. Xu L, Ma X, Sun N, Chen F. Bulk oxygen vacancies enriched TiO_2 and its enhanced visible photocatalytic performance. Appl. Surf. Sci. 2018 May; 441: 150-155. https://doi.org/10.1016/j.apsusc.2018.01.308
7. Shah MW, Zhu Y, Fan X, Zhao J, Li Y, Asim S, *et al*. Facile Synthesis of Defective TiO_{2-x} Nanocrystals with High Surface Area and Tailoring Bandgap for Visible-Light Photocatalysis. Sci. Rep. 2015 Oct; 5: 1-8. https://doi.org/10.1038/srep15804
8. Ramírez-Herrera AD, Barbosa-Sabanero G, Lazo-de-la-Vega-Monroy ML, González-Domínguez MI. *Bougainvillea spectabilis* como mediadora para la biosíntesis de nanopartículas de plata, evaluación de su efecto antimicrobiano y citotóxico. Biotecnia, 2024; 26(1): 332–341. https://doi.org/10.18633/biotecnia.v26.2257
9. Prokopiuk V, Yefimova S, Onishchenko A, Kapustnik V, Myasoedov V, Maksimchuk P, *et al*. Assessing the Cytotoxicity of TiO_{2-x} Nanoparticles with a Different Ti^{3+} $(Ti^{2+})/Ti^{4+}$ Ratio. Biol. Trace Elem. Res. 2023 Aug; 201(6): 3117-3130. https://doi.org/10.1007/s12011-022-03403-3
10. Ni W, Li M, Cui J, Xing Z, Li Z, Wu X, *et al*. 808 nm light triggered black TiO_2 nanoparticles for killing of bladder cancer cells. Mater. Sci. Eng. C 2024 Dec; 81: 252-260. https://doi.org/10.1016/j.msec.2017.08.020
11. Sun L, Li Z, Li Z, Hu Y, Chen C, Yang C, *et al*. Design and mechanism of core–shell TiO_2 nanoparticles as a high-performance photothermal agent. Nanoscale 2017 Aug; 9(42): 16183-16192. https://doi.org/10.1039/C7NR02848B
12. Cao Y, Chen J, Bian Q, Ning J, Yong L, Ou T, *et al*. Genotoxicity Evaluation of Titanium Dioxide Nanoparticles In Vivo and In Vitro: A Meta-Analysis. Toxics 2023 Oct; 11(11): 1-29. https://doi.org/10.3390/toxics11110882
13. Ramírez-Herrera AD. Nanostructured materials as potential neurotoxins [carta]. Rev. Ecuat. Neurol. 2024; 33(2): 19. https://doi.org/10.46997/revecuatneurol33200019
14. Jiménez-Mejía R, Ramírez-Herrera AD, Orozco-Ceja JA, González-Domínguez MI. Biosíntesis de nanopartículas de plata con actividad antimicrobiana por *Pseudomonas aeruginosa* ambiental. Mundo Nano. 2024; 17: 1-13. https://doi.org/10.22201/ceiich.24485691e.2024.32.69721
15. Saravanan S, Dubey RS. Optical and morphological studies of TiO_2 nanoparticles prepared by sol–gel method. Mater. Today Proc. 2021 Apr; 47: 1811-1814. https://doi.org/10.1016/j.matpr.2021.03.207
16. Haryński Ł, Olejnik A, Grochowska K, Siuzdak K. A facile method for Tauc exponent and corresponding electronic transitions determination in semiconductors directly from UV–Vis spectroscopy data. Opt. Mater. 2022 May; 127: 1-9. https://doi.org/10.1016/j.optmat.2022.112205
17. Bajić V, Spremo-Potparević B, Živković L, Čabarkapa A, Kotur-Stevuljević J, Isenović E, *et al*. Surface-modified

TiO_2 nanoparticles with ascorbic acid: Antioxidant properties and efficiency against DNA damage in vitro. Colloids Surf. B Biointerfaces, 2017 Jul; 155: 323-331. https://doi.org/10.1016/j.colsurfb.2017.04.032

18. Dai S, Wu Y, Sakai T, Du Z, Sakai H, Abe M. Preparation of Highly Crystalline TiO_2 Nanostructures by Acid-Assisted Hydrothermal Treatment of Hexagonal-structured Nanocrystalline Titania/Cetyltrimethyammonium Bromide Nanoskeleton. Nanoscale Res. Lett. 2010 Aug; 5: 1829-35. https://doi.org/10.1007/s11671-010-9720-0
19. Pedraza F, Vazquez A. Obtention of TiO_2 rutile at room temperature through direct Oxidation of $TiCl_3$. J. Phys. Chem. Solids 1999 Apr; 60(4): 445-448. https://doi.org/10.1016/S0022-3697(98)00315-1
20. Liu Y, Tian L, Tan X, Li X, Chen X. Synthesis, properties, and applications of black titanium dioxide nanomaterials. Sci. Bull. 2017 Mar; 62(6): 431-441. https://doi.org/10.1016/j.scib.2017.01.034
21. Chen S, Wang Y, Li J, Hu Z, Zhao H, Xie W, *et al.* Synthesis of black TiO_2 with efficient visible-light photocatalytic activity by ultraviolet light irradiation and low-temperature annealing. Mater. Res. Bull. 2018 Feb; 98: 280-287. https://doi.org/10.1016/j.materresbull.2017.10.036
22. Su T, Yang Y, Na Y, Fan R, Li L, Wei L, *et al*. An Insight into the Role of Oxygen Vacancy in Hydrogenated TiO_2 Nanocrystals in the Performance of Dye-Sensitized Solar Cells. ACS Appl. Mater. Interfaces 2015 Jan; 7(6): 3754-3763. https://doi.org/10.1021/am5085447
23. Huerta GE, Zepeda IQ, Sánchez BH, Colín VZ, Alfaro ME, Ramos GMdelP, *et al*. Internalization of Titanium Dioxide Nanoparticles Is Cytotoxic for H9c2 Rat Cardiomyoblasts. Molecules 2018 Aug; 23(8): 1-15. https://doi.org/10.3390/molecules23081955
24. Filippi C, Pryde A, Cowan P, Lee T, Hayes P, Donaldson K, *et al*. Toxicology of ZnO and TiO_2 nanoparticles on hepatocytes: Impact on metabolism and bioenergetics. Nanotoxicology 2014 Apr; 9(1): 126-134. https://doi.org/10.3109/17435390.2014.895437
25. Meena R, Rani M, Pal R, Rajamani P. Nano-TiO_2-Induced Apoptosis by Oxidative Stress-Mediated DNA Damage and Activation of p53 in Human Embryonic Kidney Cells. Appl. Biochem. Biotechnol. 2012 May; 167: 791-808. https://doi.org/10.1007/s12010-012-9699-3
26. Wang S, Yu H, Wickliffe JK. Limitations of the MTT and XTT assays for measuring cell viability due to superoxide formation induced by nano-scale TiO_2. Toxicol. *In Vitro* 2011 Dec; 25(8): 2147-2151. https://doi.org/10.1016/j.tiv.2011.07.007
27. Tucci P, Porta G, Agostini M, Dinsdale D, Iavicoli I, Cain K, *et al*. Metabolic effects of TiO_2 nanoparticles, a common component of sunscreens and cosmetics, on human keratinocytes. Cell Death Dis. 2013 Mar; 4: 1-11. https://doi.org/10.1038/cddis.2013.76
28. Bo Y, Jin C, Liu Y, Yu W, Kang H. Metabolomic analysis on the toxicological effects of TiO_2 nanoparticles in mouse fibroblast cells: from the perspective of perturbations in amino acid metabolism. Toxicol. Mech. Methods. 2014 Jul; 24(7): 461-469. https://doi.org/10.3109/15376516.2014.939321
29. Valentini X, Rugira P, Frau A, Tagliatti V, Conotte R, Laurent S, *et al*. Hepatic and Renal Toxicity Induced by TiO_2 Nanoparticles in Rats: A Morphological and Metabonomic Study. J. Toxicol. 2019 Mar; (1): 1-19. https://doi.org/10.1155/2019/5767012
30. Jafari S, Mahyad B, Hashemzadeh H, Janfaza S, Gholikhani T, Tayebi L. Biomedical Applications of TiO_2 Nanostructures: Recent Advances. Int. J. Nanomedicine. 2020 May; 15: 3447-3470. https://doi.org/10.2147/IJN.S249441
31. Du Kang, Guohua C, Xuyuan W. Fast charge separation and photocurrent enhancement on black TiO_2 nanotubes cosensitized with Au nanoparticles and PbS quantum dots. Electrochim. Acta. 2018 Jul; 277: 244-254. https://doi.org/10.1016/j.electacta.2018.05.014
32. Saeed M, Zubair R, Wenzhi X, Yuanzhi K, Waheed W. Tunable Fabrication of New Theranostic Fe_3O_4-black TiO_2 Nanocomposites: Dual Wavelength Stimulated Synergistic Imaging-guided Phototherapy in Cancer. J. Mater. Chem. B. 2018 Jan; 7(2): 210-223. https://doi.org/10.1039/C8TB02704H
33. Dathan P, Deepak R. A Review on Biomedical Applications of Titanium Dioxide. Trends Biomater. Artif. Organs. 2023; 37(1), 49-54.
34. Chen S, Xiao Y, Wang Y, Hu Z, Zhao H, Xie W. A Facile Approach to Prepare Black TiO_2 with Oxygen Vacancy for Enhancing Photocatalytic Activity. Nanomaterials. 2018; 8(4): 1-16. https://doi.org/10.3390/nano8040245
35. Wang M, Yunlei S, Chengji W, Yue M, Xiangjian G. Photoelectrochemical biosensor for microRNA detection based on a MoS_2/g-C_3N_4/black TiO_2 heterojunction with Histostar@AuNPs for signal amplification. Biosens. Bioelectron. 2019 Mar; 128: 137-143. https://doi.org/10.1016/j.bios.2018.12.048